Conference Proceedings

EuroSun 2014
Aix-les-Bains (France), 16 - 19 September 2014

Satellite Irradiance Based on MACC Aerosols: Helioclim 4 and SolarGIS, Global and Beam Components Validation

Pierre Ineichen

University of Geneva, Institute of environmental sciences, Energy Group

Abstract

The use of geostationary satellite observations becomes crucial, since they allow the retrieval of irradiance at the surface, with the best spatial and temporal coverage. This study, conducted on data from 12 European sites, over one year, 2013, shows the performance of two of the best irradiance satellite models using MACC project as daily aerosol data input. A preliminary performance analysis of the new McClear clear sky model is also done. Typically, the irradiance is derived with a standard deviation of 18% for the global component, and 38% for the beam with a very low bias.

Key-words: satellite derived irradiance, model validation, MACC aerosols, CSP applications

1. Introduction

The meteorological satellite images as data source to evaluate the ground irradiance components become the state of the art in the field of solar energy systems. The strongest argument is the high spatial coverage, and the fifteen minutes temporal granularity when using images from MSG. They also have the advantage to provide «real time» data used for example to assess the proper operation of a solar plant. On the other hand, long term ground data are very scarce concerning the beam irradiance. The use of secondary inputs such as for example from polar satellite data, and ground information increases significantly the precision of the algorithms, mainly for the beam component. The two evaluated models use aerosol data from the MACC project (Benedictow 2012, Mocrette 2009) on a daily basis. Following a paper from Zelenka (1998) concerning the nuggets effect, the interpolation distance to the nearest ground measurement site is limited to 10 to 30 km, depending on the irradiance parameter. This strengths the satellite derived data argument.

2. Ground data

Data from 12 European and Mediterranean sites where used to conduct the validation. The climate range covers desert to oceanic, latitude from 20°N to 60°N, and altitudes from sea level to 1580 meters. As at the present time, only the year 2013 is available for the Helioclim v4 algorithm, the validation is done on only one year. The liste of the ground sites is given in Table I. A more complete validation over a longer period, 18 sites and 6 models was published by Ineichen (2013).

The concerned parameters are the global irradiance on a horizontal plane *G* (or *GHI*) and the normal beam irradiance G_b (or *DNI*). If only the diffuse component G_d is acquired, the normal beam irradiance is evaluated by difference.

The ground data are kindly provided by the Baseline Surface Radiation Network (BSRN), the Global Aerosol Watch project (GAW), the CIE International Daylight Measurements Program (Commission internationale de l'éclairage IDMP), the Universidad Politecnica de Madrid (UMP), the Ecole National des Travaux Publiques (ENTPE) of Lyon.

High precision instruments (WMO standards) such as Kipp+Zonen CM10, Eppley PSP pyranometers, and Eppley NIP pyrheliometers, are used to acquire the data. A stringent calibration, characterization and quality

doi:10.18086/eurosun.2014.08.08 Available at http://proceedings.ises.org

control was applied on all the data by the person in charge of the measurements; the coherence of the data for all the stations was verified by the author and is described in the next section.

Tab. 1: Ground sites: coordinates, altitude, measured components, climate and source

Site	G	G_b	G_d	latitude	longitude	altitude	climate	
Cabauw (The Netherlands)	x	x	x	51.97	4.94	2	temperate maritime	BSRN
Camborne (Great Britain)	x	x	x	50.22	-5.32	22	temperate maritime	GAW
Carpentras (France)	x	x	x	44.08	5.06	100	mediterranean	BSRN
Geneva (Switzerland)	x	x		46.20	6.13	420	semi-continental	CIE
Kishinev (Moldavia)	x	x	x	47.00	28.82	205	continental	GAW
Lerwick (Great Britain)	x	x	x	60.13	-1.18	82	cold oceanic	GAW
Madrid (Spain)	x	x	x	40.45	-3.73	650	semi-arid	UMP
Tamanrasset (Algeria)	x	x	x	22.78	5.51	1400	hot, desert	BSRN
Toravere (Estonia)	x	x	x	58.25	26.46	70	cold humid	BSRN
Valentia (Ireland)	x		x	51.94	-10.25	14	oceanic	GAW
Vaulx-en-Velin (France)	x	x	x	45.78	4.92	170	semi-continental	ENTPE
Wien (Austria)	x		x	48.25	16.37	203	continental	GAW

3. Quality control

Sensor calibration is the key point for precise data acquisition in the field of solar radiation. The radiation sensors should be calibrated by comparison against a sub-standard before the beginning of the acquisition period, and then every year. Due to possible errors and inaccuracies, a post-calibration is difficult to conduct.

The validity of the results obtained from the use of measured data is highly correlated with the quality of the data bank used as reference. Controlling data quality is therefore the first step to perform in the process of validating models against ground data. This essential step should be devised properly and automated in order to rapidly detect significant instrumental problems like sensor failure or errors in calibration, orientation, leveling, tracking, consistency, etc. Normally, this quality control process should be done by the institution responsible for the measurements. Unfortunately, it is not the case at many stations. Even if some quality control procedures have been implemented, it might not be sufficient to catch all errors, or the data points might not be flagged to indicate the source of the problem. A stringent control quality procedure must therefore be adopted in the present context, and its various elements are described in what follows.

Three steps of quality control have been applied on the data before to approve them for the validation:

- **Time stamp**: this can be done by symmetry in the irradiance values for clear and stable days. The irradiance is plotted against the solar elevation, if the time stamp is correct, the rising and downward curves should follow the same path. The test can also be done on all the hourly values by plotting in a different color the morning and the afternoon values of the clearness index K_t (global irradiance normalized by the corresponding extra atmospheric value) versus the solar elevation angle. In this case, the upper limits, representing clear conditions, should show a similar pattern. A 10 minutes time shift is illustrated on Fig, 1. When these tests are fulfilled, the time stamp of the data bank can be considered as correct, and the solar geometry can be precisely calculated.

- **Calibration factor of the sensors**: this can be verified for clear sky conditions by comparison against data from a nearby station or with the help of additional measurements. For each day, the highest hourly value of G and G_b is selected from the measurements and plotted against the day of the year for two nearby sites, or for two different year for the same site on the same graph. These points are representative of the clearest daily conditions. As the highest value for each day is selected, the upper limit normally represents clear-sky conditions and should show the same values (for G, it happens that higher-than-clear-sky values are obtained under partly cloudy or scattered clouds, high-sun conditions, this is why this test should not be applied for data with time granularity lower than hourly). If the aerosol optical depth (*aod*) and the water vapor content of the atmosphere (*w*) are known, a clear sky model like Solis (Müller 2004, Ineichen 2006 and 2008a) can be used to calculate the highest irradiance, and the obtained values represented on the same graph than the measurements. Here again, the upper limit should be similar. An illustration is given on Fig. 2 where data from Carpentras are represented for four years. The upper points represent the highest irradiance hourly value for each day. The blue triangles are ground measurements, the green triangles represent the clear sky irradiance evaluated with Solis and the aeronet aerosol optical depth (the water vapor is taken from ground measurements). The lower points represent the corresponding clearness index. The graphs are given for the global irradiance on the left, and the beam component on the right.

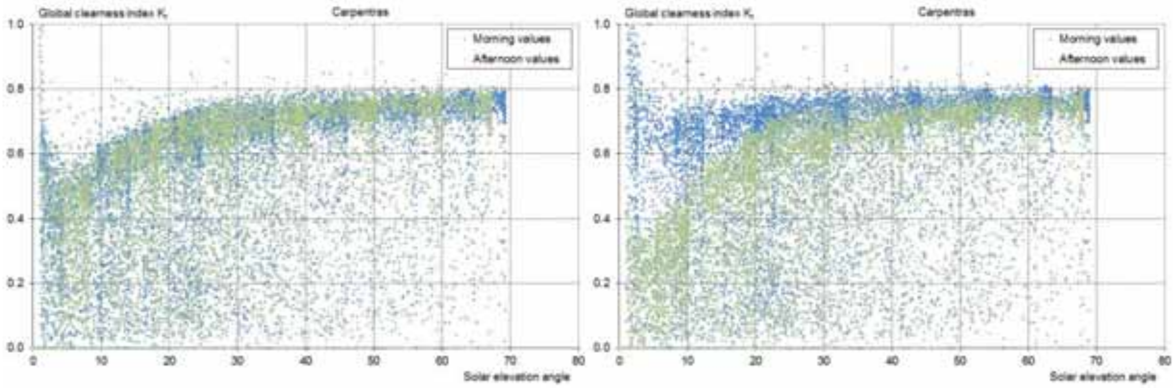

Fig 1: Time stamp validation: correct time stamp (left graph), and 10 minutes time shift (right graph)

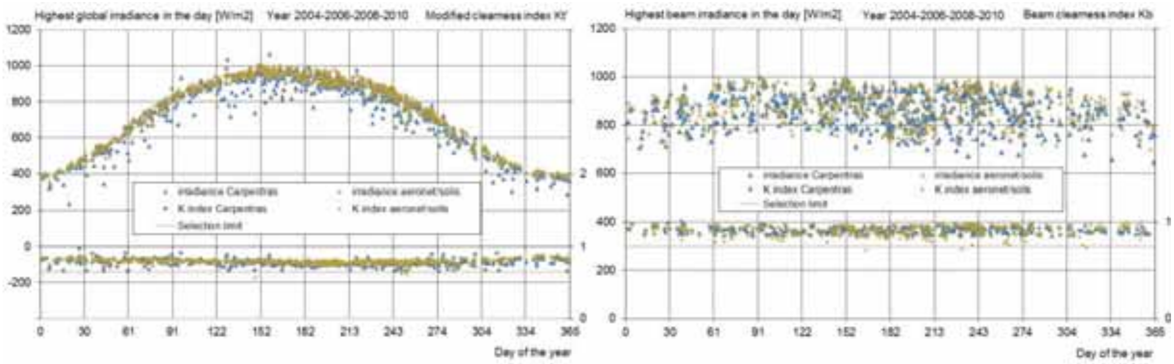

Fig 2: Highest hourly value for each day of the year for the ground measurement and the clear sky values calculated with Solis and the aeronet aod for the global (left) and the beam (right) components

- **Coherence between the components**. If the three solar irradiance components—beam, diffuse and global—are available, a consistency test can be applied, based on the closure equation that link them:

$$G_b = \frac{H - G_d}{\cos(\Theta_z)}$$

(eq. 1)

where Θ_z is the solar zenith angle. Due to the different measurement methods for each of the components, the strict equality cannot be verified for all the values and acceptability limits are to be defined.

If only the beam or the diffuse component is available, the test can be done with the help of the clearness indices or the diffuse fraction. The obtained graphs are given on Fig 3. On the same graph, the clear-sky predictions from the Solis radiative model are represented for four different a priori values of *aod*. The corresponding Linke turbidity coefficient T_{Lam2} is then calculated from the G_b thus obtained:

$$G_b = I_o \cdot e^{(-\delta_{cda} \cdot T_{Lam2} \cdot AM)}$$

(eq. 2)

where I_o is the solar constant, δ_{cda} the clear and dry atmosphere properties and *AM* the optical air mass. T_{Lam2} is evaluated for $AM = 2$ and its correspondence with *aod* is also indicated on the graph. Any important deviation between the predicted and measured clear-sky values indicates calibration uncertainties, pyrheliometer misalignment, soiled or shaded sensors, or miscategorization of clear-sky conditions.

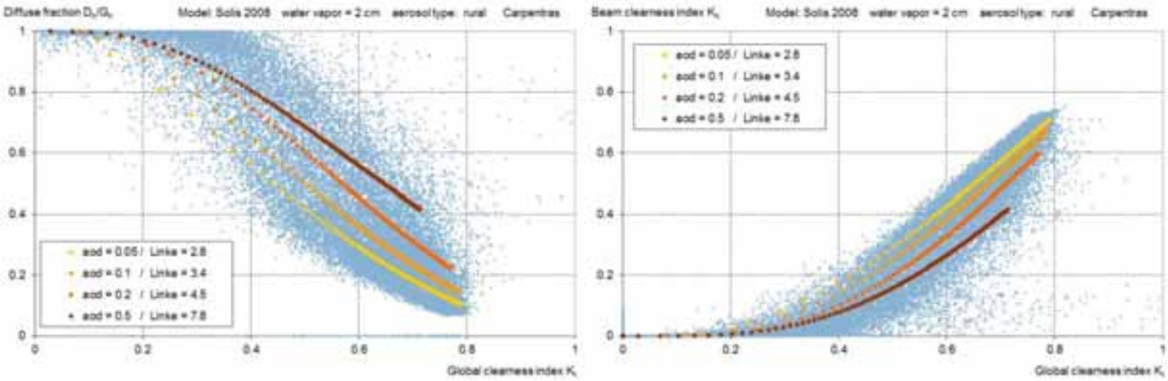

Fig. 3: Components coherence test when only the diffuse (left) or the beam (right) is available as a second component

When these conditions are fulfilled, it can be considered that the data are bankable enough to be used for the validation of the models.

4. Validation statistics

The comparison is done on an hourly, daily and monthly basis, on all the three components. The following indicators are used to describe the capability of the model to represent the measurements:

- The first order statistics: the mean bias (*mbd*), the root mean square difference (*rmsd*) and the standard deviation (*sd*). The visualization is made with the help of scatterplots of the modeled values versus the corresponding measurements.
- The dependence of the bias with the type of conditions (clear, intermediate or cloud sky), the seasons and the aerosol optical depth *aod*.
- Comparison in terms of frequency of occurrence and cumulated frequency of occurrence: for the irradiance, it gives an indication of the repartition for each level of radiation. For the clearness index, it assesses that the modeled level of radiation occurs at the right time during the day.
- The second order statistics defined by the Kolmogorov-Smirnov (*KS*) test (Zarzalejo 2009). It represents the capability of the model to reproduce the frequency of occurrence at each of the irradiance level.
- The distribution of the difference between the model and the measurements around the 1:1 model-measurements axis in term of histograms around the mean bias, and the corresponding cumulated frequency of occurrence.
- The standard deviation of the bias of all the sites. This value expresses the spatial “smoothness” of the model, or its capacity to represent any location with a minimal bias.

These statistical parameters include the dispersion due to:

- The retrieval procedure (clear sky algorithm, input parameters, cloud properties, etc.)
- The comparison of point measurements (ground data) with spatially averaged values (pixels)
- The comparison of the average of four instantaneous values (satellite images) with 60 minutes integrated ground measurements.

5. Satellite models

The two satellite models using daily values of the aerosol load of the atmosphere retrieved from the MACC project are SolarGIS from GeoModel Solar, and Helioclim-4 from Mines Paris Tech:

- **SolarGIS**: the irradiance components are the results of a five steps process: a multi-spectral analysis classifies the pixels, the lower boundary (LB) evaluation is done for each time slot, a spatial variability is introduced for the upper boundary (UB) and the cloud index definition, the Solis clear sky model is used as normalization, and a terrain disaggregation is finally applied. Four MSG spectral channels are used in a classification scheme to distinguish clouds from snow and no-snow cloud-free situations. Exploiting the potential of MSG spectral data for snow classification removed the need of additional ancillary snow data and allowed using spectral cloud index information in cases of complex conditions such as clouds over high albedo snow areas. The broadband simplified version of Solis model was implemented in the main schemes as well as in the global to beam Dirindex algorithms to calculate Direct Normal Irradiance component (Perez 1992, Ineichen 2008b). Processing chain of the model includes post-processing terrain disaggregation algorithm based on the approach by Ruiz-Arias (2010).
- **Heliosat-4**: the physical model is based on the LibRadTran radiative transfer software (Mayer 2005). Look-up tables are derived for clear and cloudy conditions and used to evaluate the shortwave irradiance components. The normalization is done with the new McClear clear sky model also developed by MinesParisTech (Lefèvre 2013). The cloud properties are derived from the Meteosat images with the APOLLO tool, and the aerosol properties, the ozone amount and the water vapor content of the atmosphere are retrieved from the MACC-II project.

6. Validation results

In a previous study, a long term validation has been conducted on time series covering up to 16 years (Ineichen 2013). The Heliosat-4 scheme covers nowadays only the year 2013; this will be the basis of the validation presented in the present paper. The performance of the previous Heliosat scheme, version 3, is also included for comparison purpose.

As an outcome from the new McClear clear sky scheme, the clearness indices have been improved from Heliosat-3 to Heliosat-4; they are now similar to SolarGIS. This is illustrated on Fig. 4 where the global clearness index K_t is represented versus the solar elevation angle for the two version of Heliosat.

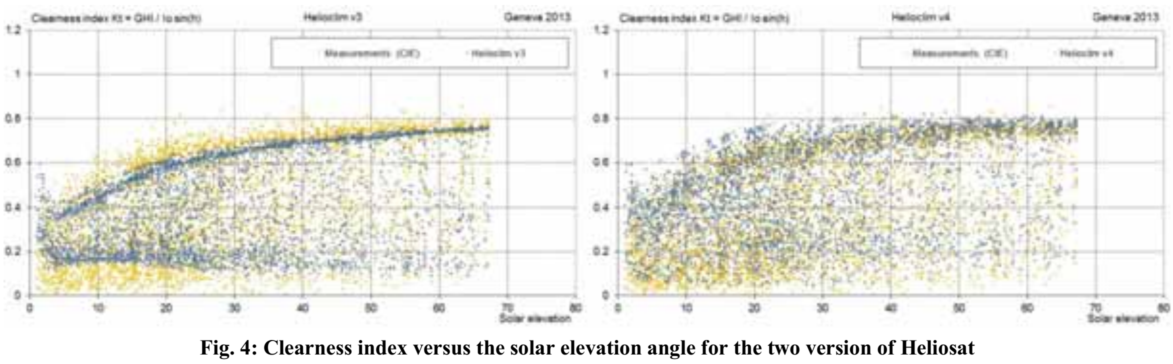

Fig. 4: Clearness index versus the solar elevation angle for the two version of Heliosat

The overall results of the validation are given in Table II in terms of bias (*mbd*), standard deviation (*sd*) and standard deviation of the bias. The first observation shows that the use of daily MACC aerosol optical depths in Helioclim-4 improves the derivation of the beam component, but reduces the performance of the global component, particularly the standard deviation of the bias.

Looking into the dependence of the bias with the clearness index and the season, the following points can be pointed out:

- The global irradiance biases are very similar for Helioclim-4 and SolarGIS, even if SolarGIS shows slightly lower dispersions,

Table II: Overall statistics of the three models for the two components

	Global irradiance								Normal beam irradiance							
			helioclim 3		helioclim 4		SolarGIS				helioclim 3		helioclim 4		SolarGIS	
	G	nb	mbd	sd	mbd	sd	mbd	sd	G_b	nb	mbd	sd	mbd	sd	mbd	sd
Cabauw 2013	254	4106	-3%	22%	12%	25%	-3%	19%	209	4106	22%	62%	-5%	57%	1%	47%
Camborne 2013	263	4151	3%	20%	11%	27%	-2%	21%	208	4151	38%	63%	-1%	61%	6%	48%
Carpentras 2013	395	3560	2%	12%	7%	15%	0%	12%	459	3560	5%	34%	-1%	25%	-1%	24%
Geneva 2013	293	4226	-3%	22%	10%	28%	2%	20%	279	4226	4%	49%	-1%	64%	5%	45%
Kishinev 2013	309	4096	3%	20%	6%	22%	6%	22%	315	4096	11%	42%	-7%	44%	-7%	44%
Lerwick 2013	201	3526	5%	31%	9%	39%	2%	30%	134	3526	65%	114%	-34%	120%	17%	97%
Madrid 2013	427	3701	1%	15%	8%	16%	1%	13%	484	3701	3%	35%	3%	27%	4%	24%
Tamanrasset 2013	618	3619	-5%	12%	-4%	11%	-10%	12%	641	3619	9%	34%	-6%	24%	-14%	26%
Toravere 2013	276	3536	-4%	27%	3%	28%	-5%	22%	301	3536	1%	63%	-31%	69%	-8%	39%
Valentia 2013	225	4474	4%	28%	14%	33%	-3%	24%	203	4474	15%	66%	-25%	68%	-21%	47%
Vaulx-en-Velin 2013	285	3899	2%	20%	14%	25%	3%	17%	278	3899	9%	47%	3%	47%	0%	36%
Wien 2013	274	4218	-3%	21%	4%	25%	-1%	20%	253	4218	5%	49%	-15%	57%	-6%	41%
All sites	315	3927	0%	19%	7%	23%	-1%	18%	308	3927	11%	49%	-8%	48%	-3%	38%
All sites absolute bias			3%		8%		4%				11%		9%		7%	
Standard dev. of the bias			4%		9%		6%				14%		12%		10%	

- Helioclim-4 performs better for the beam component and high clearness indices, but with a higher dispersion, as given on Fig. 5
- A slight seasonal pattern is present on the beam bias for SolarGIS and on the global bias for Helioclim-4, as illustrated on Fig. 6

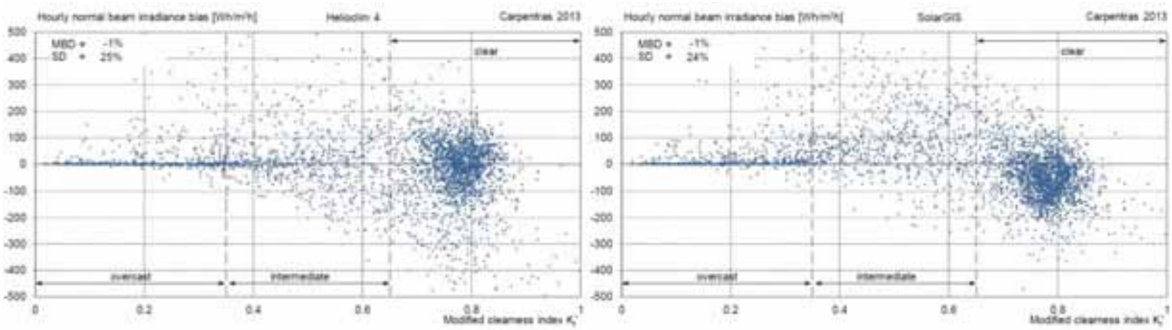

Fig. 5 Hourly data seasonal bias dependence for the normal beam irradiance at the site of Carpentras

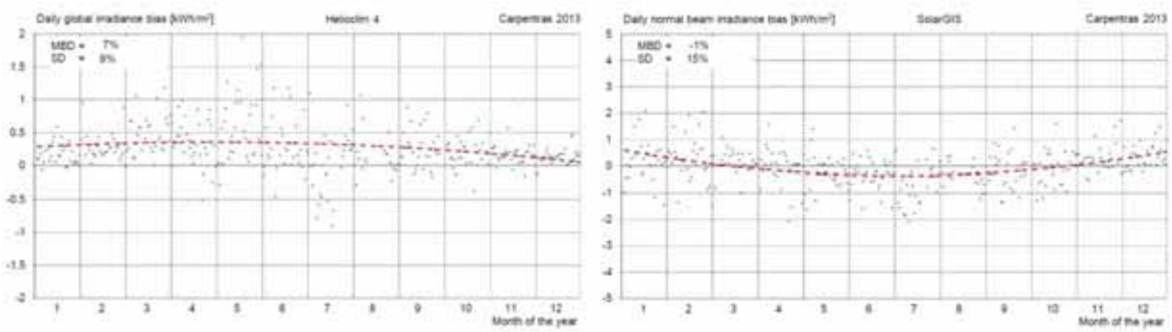

Fig. 6 Daily model seasonal bias dependence for both models at the site of Carpentras

Concerning the bias dependence with the aerosol optical depth *aod*, no particular pattern can be pointed out, neither for the beam component, nor for the global irradiance. This is illustrated on Figure. 7 for both components and the SolarGIS hourly data.

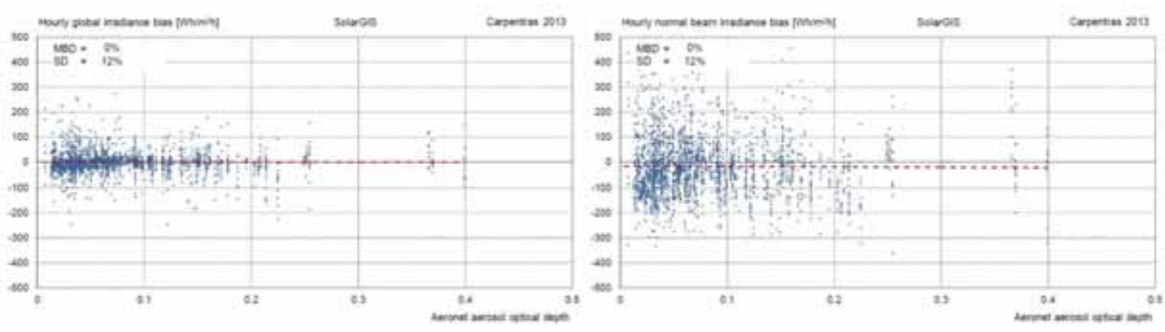

Fig. 7 Bias of SolarGIS irradiance components versus the aerosol optical depth retrieved from aeronet network

Nevertheless, the use of daily *aod* instead of climatological values shows a good improvement between version 3 and version 4 of the Helioclim data. This can be seen on Figure 8 where the beam component bias for the two versions is plotted versus the aerosol optical depth obtained from the aeronet network.

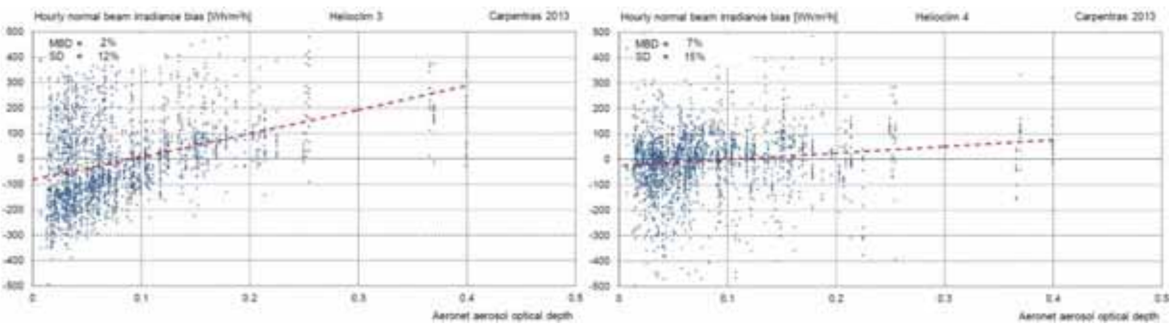

Fig. 8 Normal beam irradiance bias versus the aerosol optical depth for the two version of Helioclim

The frequency analysis is illustrated on Fig. 9 for the three models and the site of Carpentras. On these graphs the frequency of occurrence of the measurements are represented by the gray surface, and the models in different color lines. From this set of graphs, the following points can be underlined:

- For all the graphs and both components, a good improvement is obtained with Helioclim-4 compared to the version 3 of the model. This is the results of the use of daily *aod* values,
- As pointed out on Fig. 5, the frequency distribution shows a underestimation for high beam irradiances and high corresponding clearness indices for the SolarGIS data, even if the overall bias is near of zero,
- The second order statistics given by the KSI% values confirm that Helioclim-4 performs better for the beam irradiance and SolarGIS for the global component

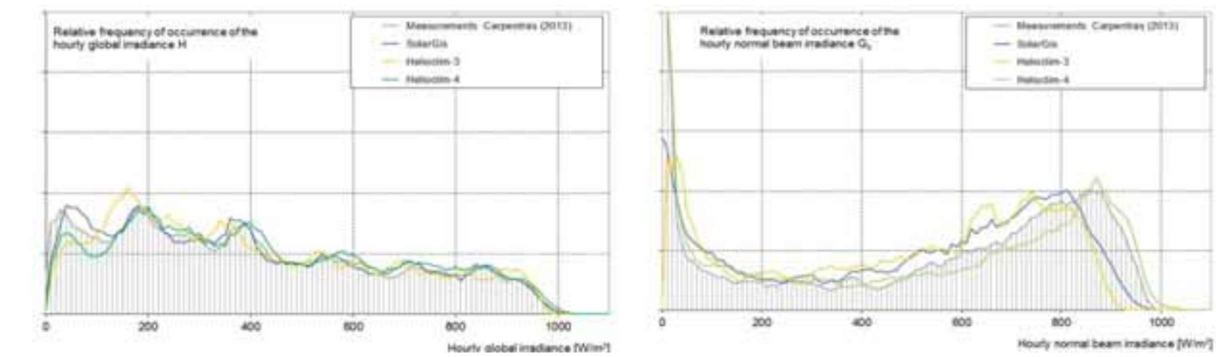

Fig. 9 Frequency of occurrence distribution of the irradiance for the global and the beam components.

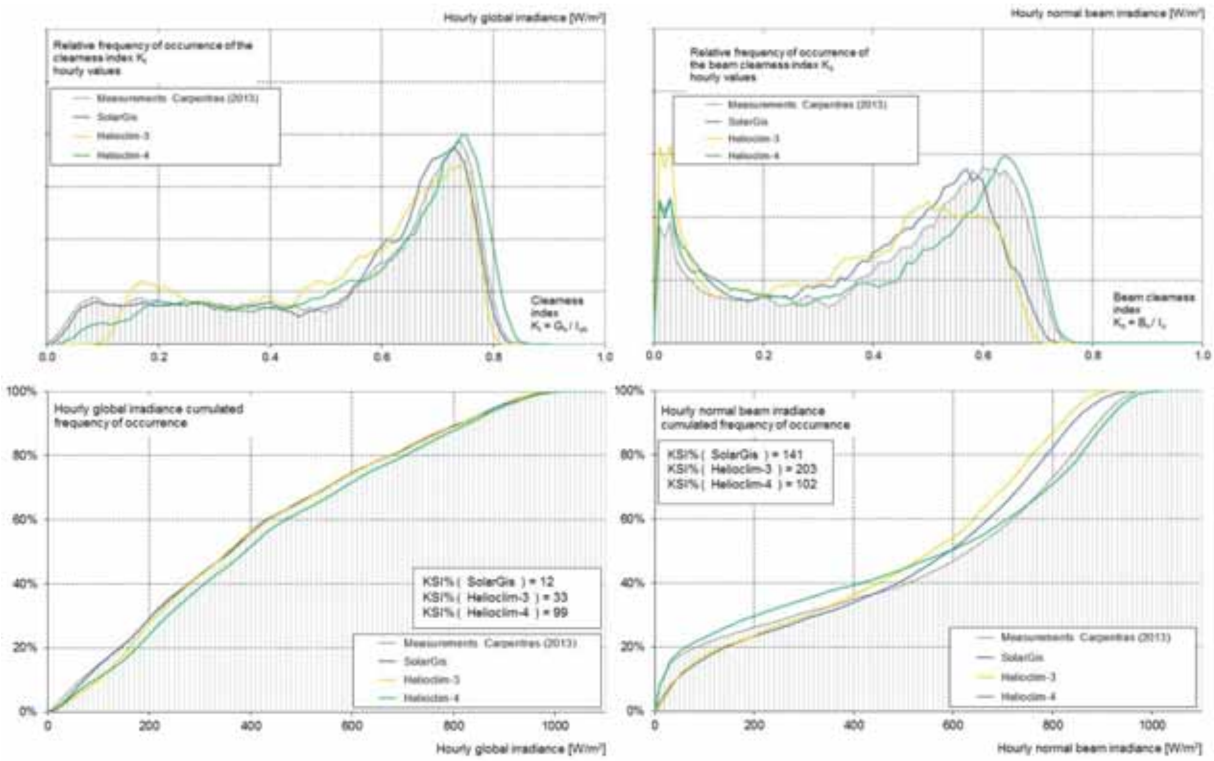

Fig. 9 (continued) Frequency of occurrence distribution of the clearness indices.
The two last graphs represent the corresponding cumulated frequency distribution

The bias frequency of occurrence around the 1:1 model-measurements axis for the global and the beam components is given on Fig. 10. The cumulated curve is also drawn on the graphs. The bar charts show that if the global irradiance bias distribution can be considered as normal, it is not the case for the beam component. Thus, the standard deviation calculated for the global component is reliable; the results for the normal beam irradiance are statistically not representative, but nevertheless, they give an idea of the dispersion.

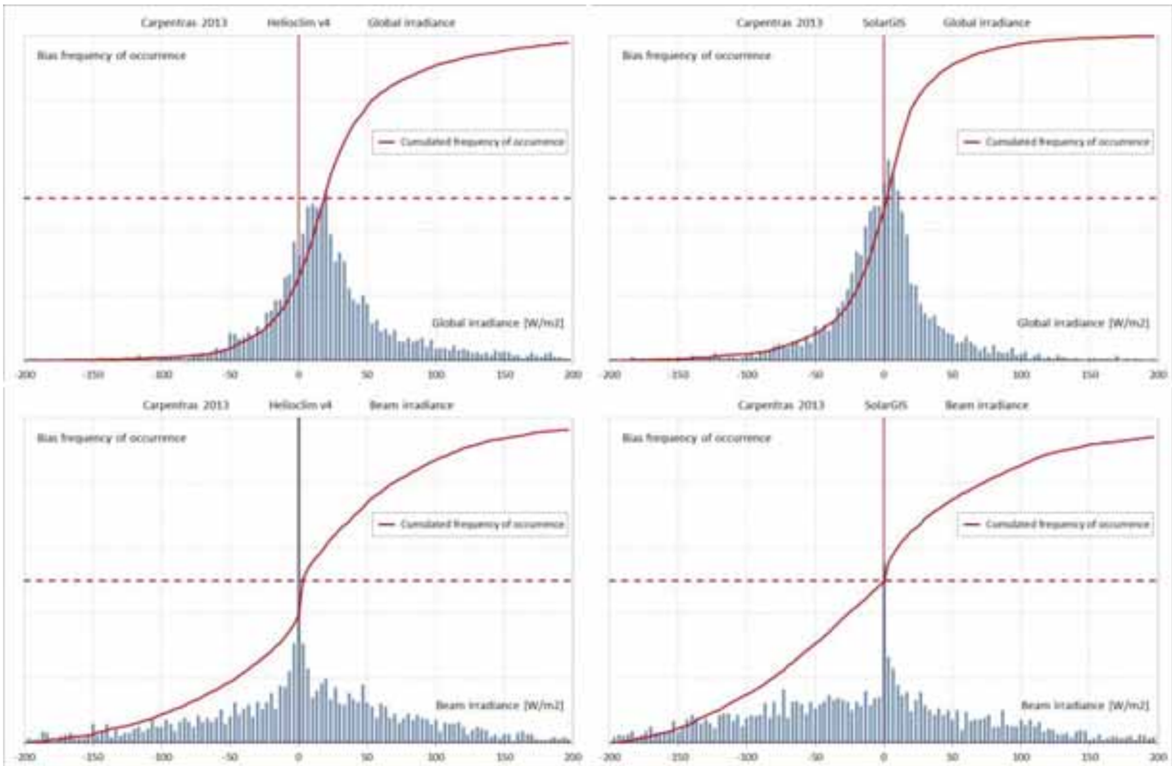

Fig. 10 Frequency distribution of the bias around the 1:1 axis for the global and the beam components

7. McClear model analysis

McClear is a new clear sky model developed by MinesParisTech (Lefèvre 2013) with daily MACC aod values as input. The author of the present paper made a short validation of the model based on the same ground data but covering the period from 2004 to 2011; this validation will be published in a next validation report. The main results are the following:

- The validation is conducted on 45'000 hourly clear sky values selected from data acquired at 18 different sites in Europe, the average global, irradiance are respectively 550 and 770 [Wh/m^{2}h]
- The global component is evaluated with a 2.7% positive bias and a 4% standard deviation, the normal beam with no bias and a 10% standard deviation. An illustration of the results site by site is given on Fig. 11,
- The bias frequency distributions around the 1:1 axis for all the components show near-normal distributions as given in Fig. 12 for the global and the beam component. This makes the first order statistics reliable,
- Seasonal pattern are present for the majority of the sites and all the components, but no generalization could be done. This will be analyzed in the McClear validation paper.

8. Conclusions

A model validation is done on one year of data from 12 European sites. Two models using MACC daily aerosol optical depths data as input are concerned: Helioclim-4 and SolarGIS. A previous Helioclim model (version 3) based on climatological Linke turbidity coefficient is given for comparison.

The main conclusion is the use of daily aerosol optical depth values as input to the algorithms is a valuable improvement to the capacity of the models to reproduce the ground measurements. The MACC project is a reliable source of these data; it has the advantage to have a high spatial coverage and resolution.

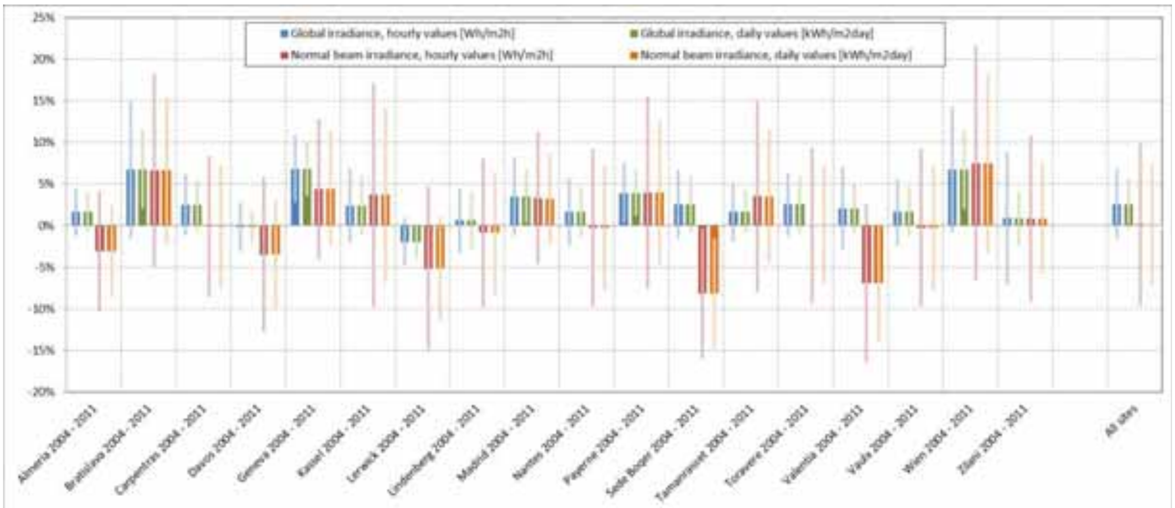

Fig. 11 First order statistics for the McClear clear sky model

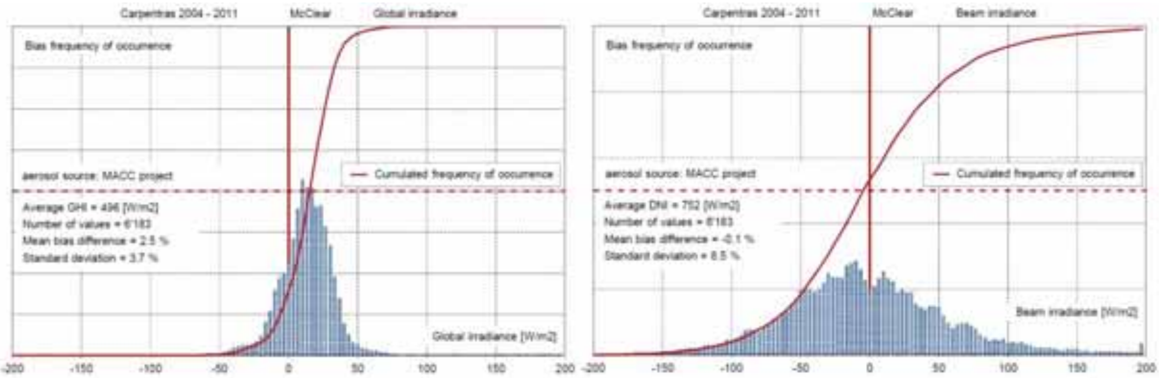

Fig. 12 Bias frequency of occurrence around the 1:1 model-measurements axis

The new McClear clear sky model gives good results over 18 European data banks covering the year 2004 to 2011; an in-depth analysis will be conducted by the author and published soon.

Helioclim-4 and SolarGIS models show specific pattern that should be evaluated and confirmed on the long term and not only on one year, here 2013. Nevertheless, the performance of SolarGIS over the year 2013 is similar to the long term analysis given in Ineichen (2013), i.e. a 18% standard deviation for the hourly global irradiance and 38% for the beam component.

9. References

Benedictow A. et al. 2012. Validation report of the MACC reanalysis of global atmospheric composition: Period 2003-2010, MACC-II Deliverable D83.1.

Ineichen P. 2006. Comparison of eight clear sky broadband models against 16 independent data banks. Solar Energy 80, pp 468–478

Ineichen P., 2008a. A broadband simplified version of the Solis clear sky model, Solar Energy 82, 758–762.

Ineichen P., 2008b. Comparison and validation of three global-to-beam irradiance models against ground measurements. Sol. Energy , doi:10.1016/j.solener.2007.12.006

Ineichen P. 2013. Long term satellite hourly, daily and monthly global, beam and diffuse irradiance validation. Interannual variability analysis. IAE Solar heating and cooling. Task 46. Geneva.

Perez R., Ineichen P., Maxwell E., Seals R., Zelenka A., 1992. Dynamic global to direct irradiance conversion models. ASHARE Trans. Res. Series, 1992, 354-369

Lefèvre M., et al. 2013. McClear: a new model estimating downwelling solar radiation at ground level in clear-sky conditions. Atmos. Meas. Tech., 6, 2403-2418, 2013, doi:10.5194/amt-6-2403-2013.

Mayer B. and Kylling A., 2005. Technical note: The libRadtran software package for radiative transfer calculations - description and examples of use. Atmos. Chem. Phys., 5, 1855-1877. doi:10.5194/acp-5-1855-2005

Morcrette J., et al. 2009. Aerosol analysis and forecast in the ECMWF Integrated Forecast System. Part I: Forward modelling. Journal of Geophysical Research, 114.

Müller, R., et al. 2004. Rethinking satellite-based solar irradiance modelling – the solis clear-sky module, Remote Sensing of Environment, 91(2), 160–174, doi:10.1016/j.rse.2004.02.009.

Ruiz-Arias J.A., Cebecauer T., Tovar-Pescador J., Šúri M. 2010. Spatial disaggregation of satellite-derived irradiance using a high resolution digital elevation model, accepted to Solar Energy.

Zarzalejo L.F., Polo J., Martín L., Ramírez L., Espinar B., 2009. A new statistical approach for deriving global solar radiation from satellite images. Solar Energy, Volume 83, Issue 4, Pages 480-484

Zelenka, A., Perez R., Seals R. and Renné D., 1998. Effective accuracy of models converting satellite radiances to hourly surface insolation. Proc. 9th Conference on Satellite Meteorology and Oceanography, Paris, 25-29 May, 1998, 710–713.